Stem Cell Research & Therapy

RESEARCH

Open Access

Mesenchymal stem cells-derived exosomes and Kaempferol improve myelin repair via attenuating inflammation and oxidative stress in a cuprizone-induced demyelination model

Fatemeh Rabiei[1,2], Hamid Askari[1,2,3], Mohammad Javan[4], Giuseppina Leo[5], Chiara Lucchi[5], Roghayeh Pourbagher[2], Giuseppe Biagini[5*] and Maryam Ghasemi-Kasman[2,6*]

Abstract

Background Exosomes (EXOs), small vesicles secreted by cells, and kaempferol (KMP) as a natural flavonoid have anti-inflammatory and anti-oxidant activities. Here, we investigated the therapeutic potential of combination therapy of mesenchymal stem cell (MSC)-derived EXOs with KMP in a cuprizone (CPZ)-induced demyelination model.

Methods Forty-five male C57BL/6J mice were used in this study. KMP was administered intracerebroventricularly and EXOs were delivered intranasally. Behavioral tests, tissue analyses, and molecular assays measured working memory, cognitive function, motor function, myelin integrity, oxidative stress, and inflammation.

Results Behavioral assessments using Y-maze, novel arm discrimination, and wire hang tests revealed that the combination therapy significantly improved working memory, spatial recognition, and motor endurance compared to KMP or EXOs treated groups. Histological analyses demonstrated marked prevention of demyelination, as evidenced by enhanced myelin integrity on FluoroMyelin and Black-Gold II staining. At the molecular level, the combined treatment up regulated the antioxidant genes expression and regulated the activity of key antioxidant enzymes, while simultaneously reducing lipid peroxidation. Glial activation and pro-inflammatory cytokine genes expression were also reduced in the EXO + KMP treated mice.

Conclusions These findings suggest that combination therapy with EXOs and KMP improves myelin repair by targeting oxidative stress and neuroinflammation in a CPZ-induced demyelination model.

Keywords Exosomes, Kaempferol, Myelin, Inflammation, Oxidative stress, Glial activation

*Correspondence:
Giuseppe Biagini
giuseppe.biagini@unimore.it
Maryam Ghasemi-Kasman
m.ghasemi@mubabol.ac.ir; maryam.ghasemi65@gmail.com
[1]Student Research Committee, Babol University of Medical Sciences, Babol, Iran
[2]Cellular and Molecular Biology Research Center, Health Research Institute, Babol University of Medical Sciences, P.O. Box 4136747176, Babol, Iran
[3]Health Policy Research Center, Institute of Health, Shiraz University of Medical Sciences, Shiraz, Iran
[4]Department of Physiology, Tarbiat Modares University, Tehran, Iran
[5]Department of Biomedical, Metabolic, and Neural Sciences, University of Modena and Reggio Emilia, Modena, Italy
[6]Department of Physiology, School of Medicine, Babol University of Medical Sciences, Babol, Iran

Introduction

One of the most common inflammatory and neurodegenerative diseases in relation with demyelination in the central nervous system (CNS) is multiple sclerosis (MS). There are currently various studies that investigated merely the demyelinated lesions and the procedures in axonal loss, however there also is a need in understanding the underlying mechanisms playing role in neurodegeneration more efficiently which has been studies in much lesser amount [1]. This demyelinative disease is known by its complex pathogenesis and different numerous pathways involved including immune-associated procedures, oxidative stress, demyelinative immunity and neural cell apoptosis [2].

Most usual therapies currently in use for MS are considered to inhibit adaptive immune system and are basically monotherapeutic immunosuppressor [3], which are divided into short-term, intermittent, and long-term. There might be immunomodulation troubles due to specific genetic deficits and acquired immune-dysregulation which will be followed by an increase in the autoimmune system activity [4, 5]. Thus, a multifaceted therapeutic approach that addresses both inflammatory and oxidative pathways is needed to improve the partially effective currently available MS therapies. One of the potential strategies that have been considered recently is combining two or more drugs in the context of MS which can impact on different individuals pathways simultaneously and exhibit synergistic efficiency [6].

Exosomes (EXOs) as small extracellular membrane-bound vesicles have numerous therapeutic applications. Understanding this extracellular vesicle requires to concentrate on its related components and molecular-associated pathways. EXOs have a lipid bilayer for endurance and stability, which maintains their biological potential and it also protects from external degradation. The lipid bilayer is also hosting several, different molecules, including fatty acid-binding proteins, arachidonic acid, phosphatidic acid, etc. Additionally, enzymes, cytokines, and microRNAs (miRNAs), which contribute to cellular homeostasis and may develop therapeutic effects, are found in the EXOs [7, 8]. Drug delivery systems, with EXOs hold promising potential regarding targeted therapies in the context of MS. Their specific ability to cross the blood-brain barrier (BBB) easily and deliver loaded agents to CNS makes them especially ideal as a nanocarrier for drug delivery. There are studies available which investigated EXOs efficiency in the context of MS through remyelination promotion, inflammation suppression, and also immune activity modulations [9]. In MS patients, it was shown that EXOs are capable in transporting specific markers that leads to immunity activation and inflammatory responses which progresses the disease in the CNS [10, 11].

Kaempferol (KMP) is a natural flavonoid found in various plants, spinach, tea, broccoli, etc. that acts as a secondary metabolite [12, 13]. KMP showed different pharmacodynamics including anti-depression, anti-inflammation, and specifically anti-apoptotic therefor anti-tumor activities [14, 15]. There have been extensive researches regarding KMP and its anti-oxidative aspects both in vitro and in vivo [16]. It was found that it leads to destruction of free radicals and reactive oxygen species (ROS), thus mitigating transformation of cells into malignant types and inhibiting inflammatory pathways [17]. Based on the mechanisms that contributes to MS pathogenesis and the different parallel pathways that either EXO and KMP plays their role in, these actions may act as a complementary preformation by impacting on oxidative stress and neuroinflammation in the context of MS.

Our study aimed to evaluate the combined effects of MSCs-derived EXOs and KMP to simultaneously target inflammatory and oxidative pathways in a cuprizone (CPZ)-induced demyelination model. We aimed to assess the effects of this dual-target strategy on behavioral parameters, neuroinflammation, oxidative stress, and remyelination in the corpus callosum of the mice.

Materials and methods

Chemicals and reagents

DMEM/F12 medium, fetal bovine serum (FBS), penicillin/streptomycin mixture (P/S), trypsin–EDTA, and sucrose were obtained from Biowest (France) and Merck (Germany), respectively. CPZ and KMP (≥ 97% purity) were purchased from Sigma Aldrich (St.Louis, MO, USA).

Isolation of MSCs from rat bone marrow tissue following EXO isolation

Bone marrow MSCs were extracted from femurs and tibias of four Sprague-Dawley rats, plated in DMEM/F12 + 10% FBS + antibiotics at 37 °C/5% CO_2, and passaged at 80–90% confluence with 0.05% trypsin/0.02% EDTA. For EXOs extraction, P4 cells were serum starved 24 h, the medium was 0.22 µm filtered, mixed overnight with Exocib reagent, centrifuged (3000×*g*, 40 min), resuspended in phosphate-buffered saline (PBS), and stored at -80 °C until use.

EXO characterization was confirmed in our previous report [18], where morphology was visualized by transmission electron microscopy (TEM), size distribution was analyzed by dynamic light scattering (DLS), EXO-related markers (CD9, CD63, CD81, calnexin) were validated by Western blotting, and protein concentration was quantified using the Bicinchoninic acid (BCA) assay. Representative images and validation data are available in the mentioned study [18].

EXO localization in the brain of mice

For tracking of EXOs in the brain of mice, 1 mL of EXOs was labeled with 10 µL of 20 mM Dil (Invitrogen) for 20 min, re-isolated with the Exocib reagent, adjusted to 150 mg/mL, and injected intravenously into C57BL/6J mice that were fed a 0.2% CPZ diet for 8 weeks (n = 3). After 24 h, brains were fixed in 4% paraformaldehyde (PFA) overnight, cryoprotected in 30% sucrose for 48 h, sectioned at 7 µm, and analyzed by an Olympus microscope IX71 (Japan) [19].

Animals

Forty-five male C57BL/6J mice (6–8 weeks old, 25–30 g) were purchased from Pasteur Institute of Iran (Tehran, Iran) and housed at 22 ± 2 °C and 55 ± 10% humidity on a 12 h light/dark cycle with free access to food and water. All procedures were approved by the Ethics Committee of Babol University of Medical Sciences (IR.MUBABOL.AEC.1402.019) and adhered to the *NIH Guide for the Care and Use of Laboratory Animals* and ARRIVE guidelines. Maximum effort was made to minimize distress and reduce animal numbers.

Experimental groups

To induce demyelination, C57BL/6 mice were fed a diet containing 0.2% (w/w) CPZ for 8 weeks, after which the CPZ was removed. Forty-five mice (n = 9) were randomly assigned to the following groups:

Group 1 served as the healthy control group and received no interventions.

Group 2 received CPZ at 0.2% (w/w) for 8 weeks, followed by intranasal PBS (vehicle) twice during the 2 weeks post-CPZ cessation and 5% DMSO administered via an intracerebroventricular (ICV) cannula at the beginning of weeks 9 and 10 [20]. **Group 3** received CPZ at 0.2% (w/w) for 8 weeks, followed by the intranasal administration of BM-MSC EXO (10 µg per administration) four times over 2 weeks [21].

Group 4 received CPZ at 0.2% (w/w) for 8 weeks, followed by the administration of KMP (40 µg/µL) via an ICV cannula at the beginning of weeks 9 and 10.

Group 5 received CPZ at 0.2% (w/w) for 8 weeks, followed by concurrent intranasal administration of BM-MSC EXOs (10 µg, four times over 2 weeks) and ICV administration of KMP at the beginning of weeks 9 and 10. Number of animals for each experiment was chosen based on our previous reports [18, 22].

Behavioral tests including Y-maze and novel arm discrimination test (NADT) were performed on day 0 (pre-CPZ), days 57–58 and days 72–73 . The wire hang test was done on day 74. After behavioral assessments, the animals were euthanized by intraperitoneal injection of ketamine (100 mg/kg) and xylazine (10 mg/kg). Then, the brain tissues were collected for gene expression, histological, and biochemical analyses. Figure 1A shows a schematic design of the experiments.

Stereotaxic surgery

For the ICV injections of KMP or its vehicle, the mice were anesthetized intraperitoneally with ketamine (100 mg/kg) and xylazine (10 mg/kg) during the seventh week of CPZ administration. Then, they secured in a stereotaxic device, and the scalp was incised. A cannula was then implanted into the right lateral ventricle at bregma referenced coordinates: AP: − 0.5 mm, ML: +1.8 mm, DV: − 2.0 mm.

Y-Maze test

The Y-maze test was conducted in a low-light, quiet room over an 8 min period, during which arm entries were approved once the mouse's tail base crossed the arm threshold. Sequences of three consecutive, non-repeated arm entries (e.g., ABC, BCA) were included to calculate spontaneous alternation (%) as [23]:

$$\text{Spontaneous alternation}\,(\%) = \frac{\text{Number of spontaneous alterations} \times 100}{\text{Total arm entries} - 2}$$

Novel arm discrimination test (NADT)

NADT was assessed in a two-step Y-maze: during the 3 min acquisition trial one arm was blocked while mice explored the other two, and after a 30 min interval the novel arm was unblocked for a 3 min retention trial. The maze was wiped with 10% alcohol between sessions, and spatial memory was quantified as the percentage of time spent in the novel arm, and the percentage of novel arm entries [24].

Wire Hang test

Grip strength and endurance were measured by placing mice with their forepaws on a 1.5 mm wire suspended 30 cm above a soft surface. The hanging time for up to 3 min (ends after three consecutive falls), total hanging time, the number of full wire reaches, and latency to their third fall were measured for each mouse [25].

Quantitative real-time PCR (qRT-PCR) analysis

To assess myelination, oxidative stress, and inflammatory markers, the corpus callosum was dissected from brain samples. Total RNA was isolated via a Total RNA Extraction Kit (ParsTous Co., Iran), and the RNA concentration was verified via a NanoDrop spectrophotometer. cDNA synthesis was carried out from 1 µg of total RNA with the Easy cDNA Supra-TM Synthesis Kit (ParsTous Co., Iran). cDNA purity was confirmed via a NanoDrop spectrophotometer. qRT-PCR was performed in duplicate

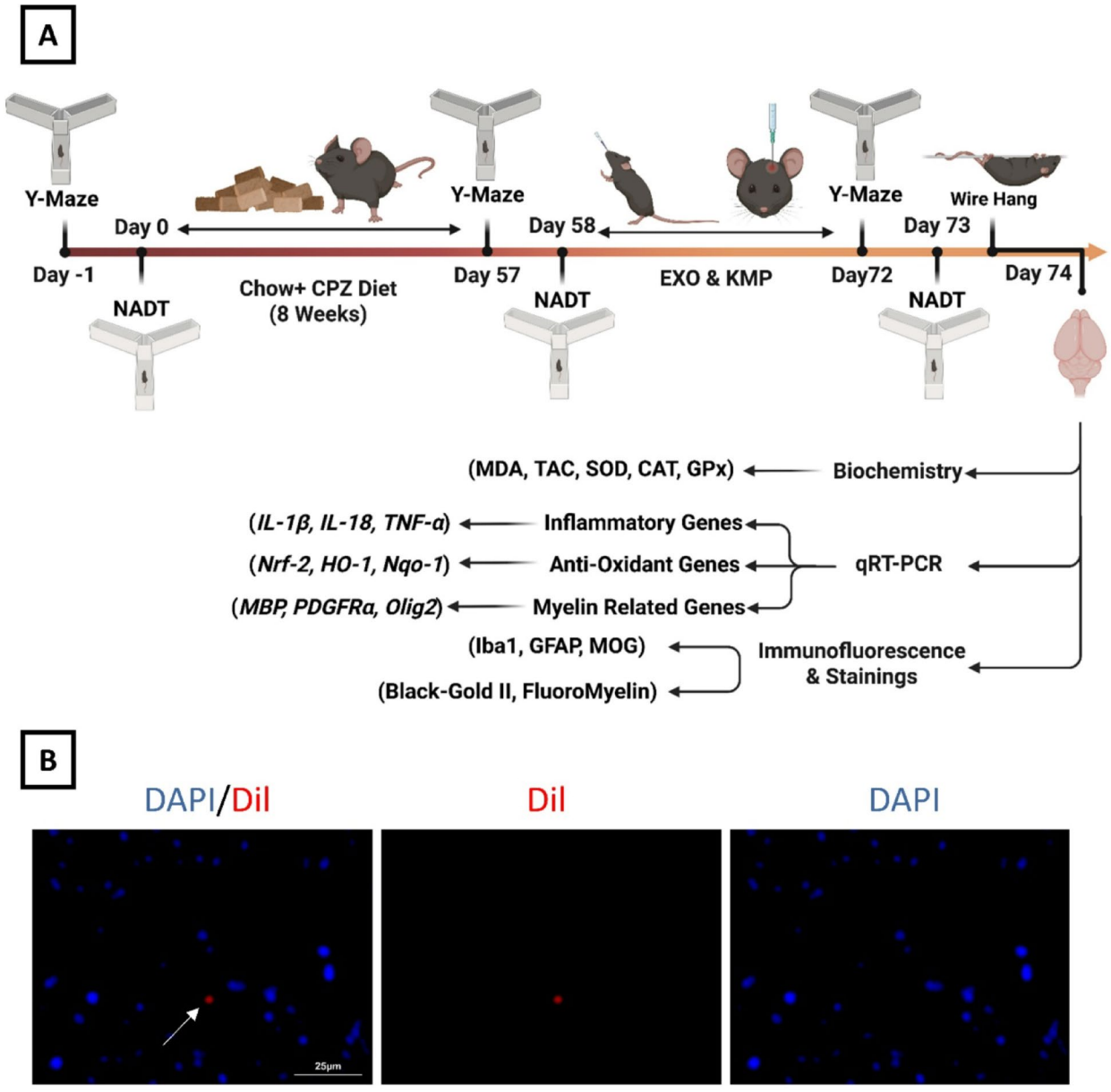

Fig. 1 Brain localization of EXOs. **A** Experimental design of the study. **B** Localization and detection of EXO-DiI (red) beside the cell nucleus (blue) in the brains of CPZ-treated mice for 8 weeks. Scale bar: 25 μm

with SYBR® Green PCR Master Mix (Ampliqon Co., Denmark) for nine target genes: *TNF-α*, *IL-18*, *IL-1β*, *MBP*, *Olig2*, *PDGFα*, *Nrf2*, *Nqo-1*, and *HO-1*. Each PCR mixture included 7.5 μL of SYBR Green, 1.5 μL of cDNA, 5.2 μL of nuclease-free water, and 0.8 μL of primer mixture (forward/reverse). *Eef2* served as the housekeeping gene. Gene expression fold changes were calculated via the $2^{-\Delta\Delta CT}$ method relative to the control group [26]. Table 1 shows the sequence of primers.

Biochemical assays

The brain tissue samples (20 mg) were homogenized in PBS, centrifuged at 12,000 rpm for 15 min, and the supernatant stored at −70 °C. The Malondialdehyde (MDA), total antioxidant capacity (TAC), superoxide dismutase (SOD), and catalase (CAT) activities and glutathione peroxidase (GPx) were then measured using biochemical assays (Kiazist Co., Iran) per the supplier-written protocol [22].

Immunofluorescence

Mice were anesthetized with ketamine (100 mg/kg) and xylazine (10 mg/kg), perfused with PBS and 4% PFA. The brain samples were post-fixed in PFA (14–16 h), cryoprotected in 30% sucrose (24–48 h), then coronally sectioned at 7 μm via a cryostat (Leica, Germany). Sections

Table 1 The sequences of primers used in the present study

Gene	5′ Forward 3′	3′ Reverse 5′	Gene bank accession number	Product length (bp)
Nrf2	CCAGCACATC-CAGACAGA-CACC	GGCAAGC-GACTCATGGT-CATCTAC	NM_010902	2347
HO-1	TGAACACTCTG-GAGAT-GACACCTG	CTGT-GAGGGACTCTG-GTCTTTGTG	NM_010442	1634
Nqo-1	CAGCCAAT-CAGCGTTCG-GTATTAC	AGCCTCTACAG-CAGCCTCCTTCA	NM_008706	1552
MBP	CAGAGACAC-GGGCATCCTT-GAC	GCAGGGAGC-CATAATGGG-TAGTTC	NM_001025245	4820
Olig2	CTTATTACAGAC-CGAGCCAA-CACC	GACGATGGGC-GACTAGACACC	NM_016967	2462
PDGFRα	AAGTG-GAAGAGAC-CATCGCAGTTC	TGTGAGTTCA-GATCG-CAGAGTGG	NM_001347719	4087
IL-18	CGCCT-CAAACCTTC-CAAATCACTTC	CAAAGTTGTCT-GATTCCAG-GTCTCC	NM_001357222	1013
IL-1β	ATGCCACCTTTT-GACAGTGAT-GAG	ATGTGCTGCT-GCGAGATTT-GAAG	NM_008361	1348
TNF-α	CATCTTCT-CAAAATTC-GAGTGACAA	TGGGAGTAGA-CAAGGTA-CAACCC	NM_001278601	1605
Eef2	CTTCCCT-GTTCACCTCT-GAC	TGATGGCACG-GATCTGATCT	NM_007907	3074

were permeabilized, blocked, incubated overnight with primary antibodies against GFAP (Z0334, Dako, 1:2000 dilution), Iba1 (019-19741, Wako, 1:1000), and MOG (MAB5680, Millipore, 1:200), followed by (goat anti-rabbit IgG (H+L) cross-adsorbed secondary antibody, Alexa Fluor™ 594 (A-11012), and goat anti-rabbit IgG (H+L) cross-adsorbed secondary antibody Alexa Fluor™ 488 (A-11008), Invitrogen, 1:1000), conjugated secondary antibodies, mounted with 20 µL of DAPI-containing Ultra-Cruz™ mounting medium (Santa Cruz Biotechnology Inc., CA, sc-24941), and examined by fluorescence microscopy (Y-TV55, Nikon, Japan) [22]. In this study, three animals per group were used for quantification of histological data in accordance with previous reports [27, 28].

FluoroMyelin staining

Tissue sections were washed, stained with FluoroMyelin (Thermo Fisher Scientific, Waltham, MA, USA) for 20 min at room temperature, rinsed, and imaged by fluorescence microscopy (Y-TV55, Nikon, Japan) to quantify demyelination extent in the corpus callosum as we mentioned in the previous report [22].

Black-Gold II staining

Black-Gold II (Merck Millipore, Germany) staining was performed by drying frozen sections, incubating them in heated staining solution for 12 min, rinsing, fixing in 1% sodium thiosulfate, washing, dehydrating, clearing, then images were captured using a bright-field microscope (C-TEP3, Nikon, Japan) [29].

Statistical analysis

Data analysis was performed using GraphPad Prism 9. Normality of data was checked via the Shapiro Wilk test. The Y-maze and NADT data were assessed by repeated-measures analysis with Bonferroni post hoc test, while the wire hang, biochemical, histological, and genes expression results were analyzed using one-way ANOVA followed by Tukey post-test. Significance was set at $P < 0.05$.

Results

EXO localization

In our study, EXO localization was performed to determine the distribution of EXOs in the target brain area, which is the corpus callosum, of the mice. As shown in Fig. 1B, the red fluorescence from EXOs-Dil clearly indicates the presence of EXOs, and the blue DAPI staining indicates the presence of cell nuclei.

EXO and KMP combination therapy reverses behavioral deficits in cuprizone-induced demyelinated model

First, the effects of EXOs and KMP on the working memory process in the CPZ-induced demyelination model were investigated. Three separate timelines, i.e., before CPZ administration, 8 weeks after CPZ application, and 2 weeks after receiving treatment, were used for the Y-maze behavioral test. The results revealed that, on day 57, spontaneous alternation decreased in all the CPZ-treated groups compared with the intact group (intact vs. CPZ + Vehicle, intact vs. CPZ + EXO and intact vs. CPZ + EXO + KMP: $P < 0.0001$, intact vs. CPZ + KMP: $P = 0.0006$). On day 72, after EXO and KMP treatment, the results of the Y-maze data indicated that the percentage of spontaneous alternation, which is an indicator of short-term memory, significantly increased in the CPZ + EXO ($P = 0.0032$), CPZ + KMP ($P = 0.0008$), and CPZ + EXO + KMP ($P < 0.0001$) groups compared with the control group. There was no significant difference between the intact group and the co-administered group ($P > 0.9999$). Despite the significant increase in the CPZ + KMP group compared with the CPZ + Vehicle group, significant differences were still observed compared with both the intact group ($P = 0.0074$) and the

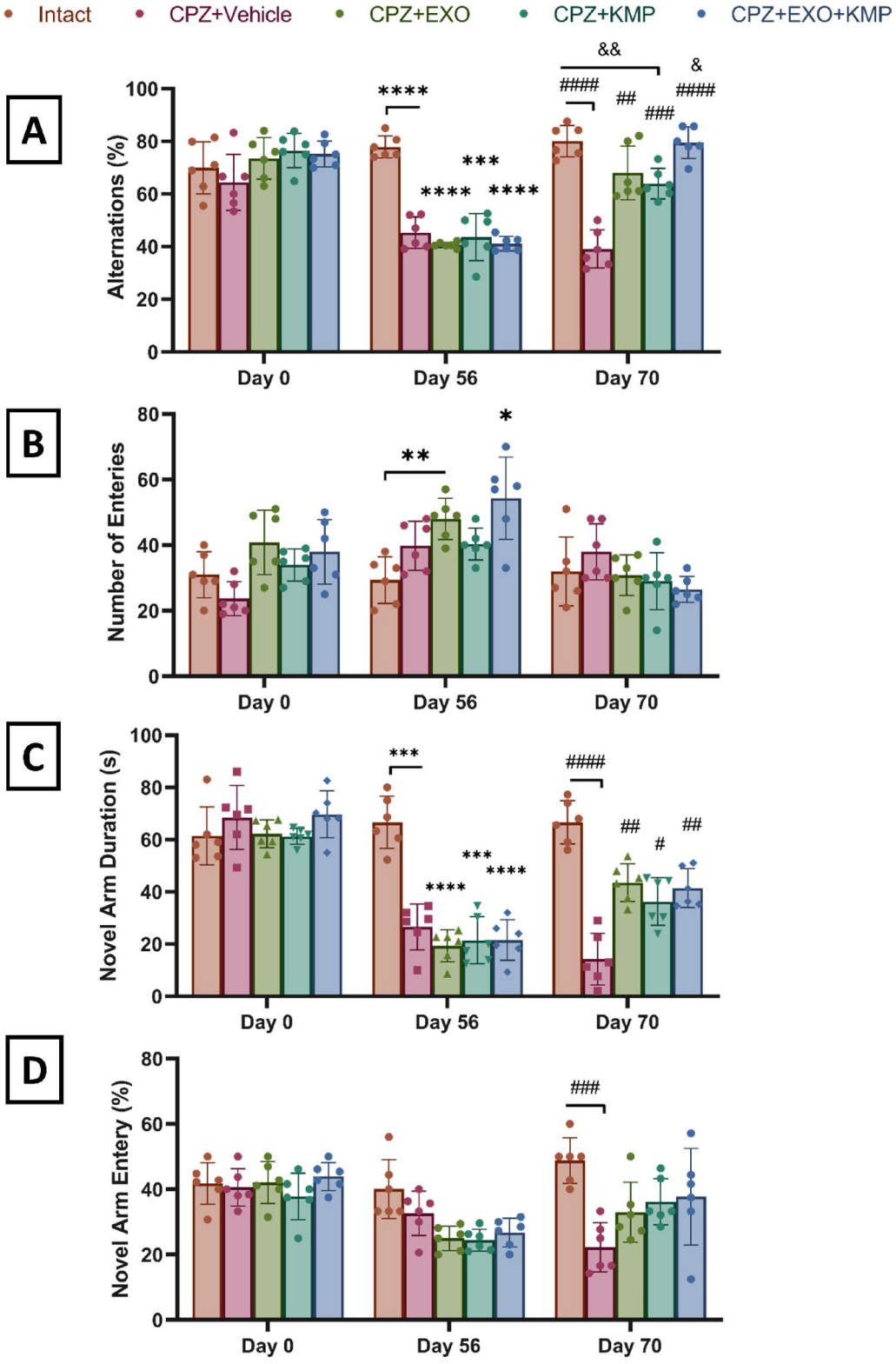

Fig. 2 (See legend on next page.)

(See figure on previous page.)

Fig. 2 Effects of EXO and KMP administration on working memory and cognitive function in a CPZ-induced demyelination model. **A** Analysis of the percentage of spontaneous alternations in the Y-maze test. On day 57 (post-CPZ), all CPZ-treated groups presented fewer alternations than the Intact group did. On day 72 (post-treatment), alterations significantly increased in the CPZ + EXO group, CPZ + KMP group, and CPZ + EXO + KMP group compared with the CPZ + Vehicle group. **B** Analysis of total arm entries. **C** Analysis of novel arm exploration duration. On day 58, all groups exhibited reduced exploration compared with the Intact. On day 73, exploration increased in the CPZ + EXO group. **D** Analysis of novel arm entries. Compared with that in the intact group, a reduction in all the CPZ-treated groups was found on day 58, but these data were not significant. On day 73, an increase was observed between the intact group and the control group. $^{*}P < 0.05$, $^{**}P < 0.01$, $^{***}P < 0.001$, and $^{****}P < 0.0001$ compared with the Intact; $^{\#}P < 0.05$, $^{\#\#}P < 0.01$, $^{\#\#\#}P < 0.001$, and $^{\#\#\#\#}P < 0.0001$ compared with the CPZ + Vehicle; $^{\&}P < 0.05$ and $^{\&\&}P < 0.01$ compared with the CPZ + KMP. Data are mean ± SEM; number of animals per group = 6

CPZ + EXO + KMP ($P = 0.0100$) group (interaction F (8, 50) = 19.10, $P < 0.0001$; time F (1.883, 47.08) = 89.37, $P < 0.0001$; treatment F (4, 25) = 26.93, $P < 0.0001$; Fig. 2A).

The total number of arm entries, which indicates memory impairment, increased across all groups on day 57; however, only the CPZ + EXO ($P = 0.0073$) and CPZ + EXO + KMP ($P = 0.0295$) groups exhibited a statistically significant increase compared with the intact group. Conversely, on day 72, the number of arm entries decreased in all treated groups, with no statistically significant differences observed relative to the intact group (interaction F (8, 50) = 9.468, $P < 0.0001$; time F (1.829, 45.71) = 31.07, $P < 0.0001$; treatment F (4, 25) = 2.327, $P = 0.0840$; Fig. 2B).

The results of both the duration of exploration and the number of entries into the novel arm in the Y-maze test indicate different patterns in the effects of the treatment interventions on the cognitive and motor abilities of the animals. On day 58, a significant decrease in the duration of exploration into the novel arm was found in all groups compared with the intact group (intact vs. CPZ + EXO and intact vs. CPZ + EXO + KMP: $P < 0.0001$; intact vs. CPZ + Vehicle: $P = 0.0003$; intact vs. CPZ + KMP: $P = 0.0001$). However, on day 73, a significant improvement in the duration of exploration to the novel arm was observed in the CPZ + EXO ($P = 0.0023$), CPZ + KMP ($P = 0.0250$) and CPZ + EXO + KMP ($P = 0.0041$) groups compared with the CPZ + Vehicle group. These results indicate the effectiveness of the treatments in improving the cognitive and motor abilities of the mice over a longer period of time (interaction F (8, 50) = 16.03, $P < 0.0001$; time F (1.671, 41.77) = 123.9, $P < 0.0001$; treatment F (4, 25) = 30.11, $P < 0.0001$; Fig. 2C).

In terms of the number of entries into the novel arm compared with the intact arm, a reduction in all CPZ-treated groups was found on day 58, but these data were not significant. On day 73, a significant increase was observed between the intact and CPZ + Vehicle groups ($P = 0.0009$). Although the treated groups also exhibited an increase, the change did not reach statistical significance compared with that of the CPZ + Vehicle group ($P = 0.0009$) (interaction F (8, 50) = 3.850, $P = 0.0014$; time F (1.876, 46.91) = 17.61, $P < 0.0001$; treatment F (4, 25) = 8.022, $P = 0.0003$; Fig. 2D).

EXO and KMP combination therapy reverses motor impairments in cuprizone-induced demyelinated model

In the Wire Hang reach score analysis on day 74, we observed a significant difference in the CPZ + Vehicle ($P = 0.0009$) and CPZ + KMP ($P = 0.0016$) groups compared with the intact group, but no significant difference was found in the CPZ + EXO ($P = 0.0725$) and CPZ + EXO + KMP ($P = 0.1777$) groups, which indicates that potential EXO and combination therapy improved neuromuscular strength (F (4, 25) = 6.907, $P = 0.0007$; Fig. 3A).

The latency test on day 74 revealed a highly significant difference between the intact and CPZ + Vehicle groups, indicating that CPZ induced motor coordination impairment. A significant improvement was observed only in the combination group ($P = 0.0198$) compared with the CPZ + Vehicle group. Furthermore, the combination group demonstrated a significant increase in time spent on the bar compared with the KMP group ($P = 0.0107$), suggesting a reinforcing effect of the two agents. Notably, the groups treated with EXOs alone ($P = 0.0434$) or KMP alone ($P < 0.0001$) also significantly differed from the intact group. (F (4, 25) = 11.36, $P < 0.0001$; Fig. 3B).

EXO and KMP combination therapy mitigates demyelination in cuprizone-induced demyelination model

FluoroMyelin staining was used to assess the extent of demyelination in the corpus callosum. Extensive demyelination was observed in the corpus callosum following CPZ-induced demyelination (Fig. 4A). There was a significant decrease between the EXO-only treatment group and the CPZ + Vehicle group ($P = 0.0142$). In addition, the extent of the demyelinated area in the EXO + KMP-treated group was significantly lower ($P = 0.0067$) than that in the CPZ + Vehicle group (F (3, 8) = 8.873, $P = 0.0063$; Fig. 4C).

In this study, the intensity level of myelin oligodendrocyte glycoprotein (MOG) in the corpus callosum was also evaluated (Fig. 4B). MOG is a myelin-specific glycoprotein that plays an important role in maintaining the stability of the myelin sheath and the function of oligodendrocytes. The results revealed that induction of demyelination with CPZ significantly reduced MOG intensity in the CPZ + Vehicle group compared with the intact group ($P = 0.0002$). There was a significant difference in

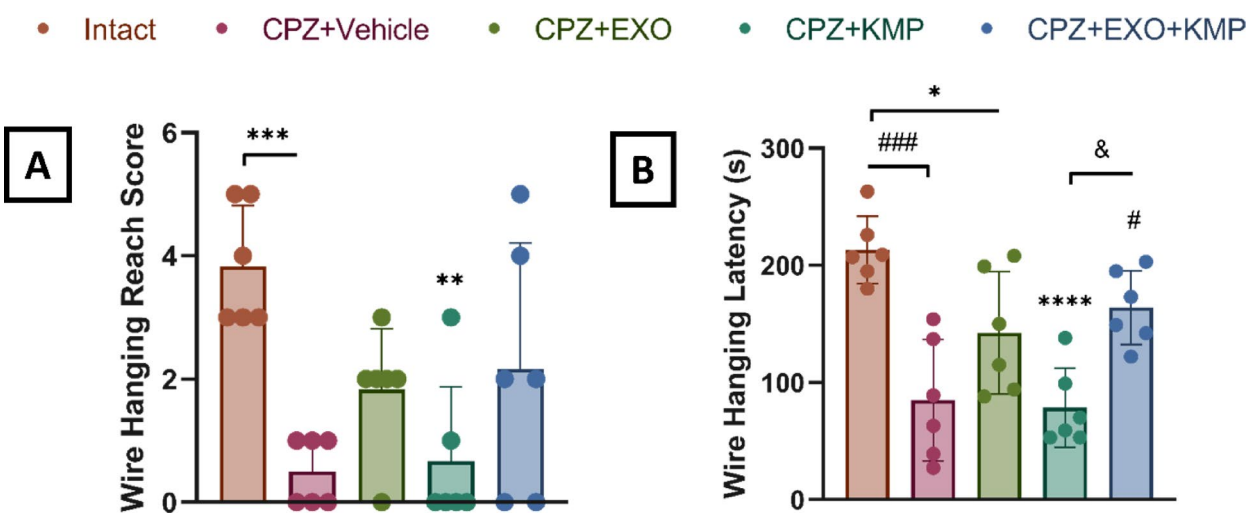

Fig. 3 EXO and KMP combination therapy reverses motor impairments in a cuprizone-induced demyelination model. **A** Analysis of wire hang reach scores on day 74. Compared with the Intact group, the CPZ + Vehicle and CPZ + KMP groups presented significant deficits in the wire hanging reach score. **B** Analysis of latency (time spent on the bar). Compared with the CPZ + Vehicle group, the CPZ + EXO + KMP group demonstrated increased latency and CPZ + KMP group, with no difference from the Intact group. CPZ + EXO and CPZ + KMP compared to the Intact group. $^{*}P < 0.05$, $^{**}P < 0.01$, and $^{***}P < 0.001$ compared with the Intact; $^{\#}P < 0.05$ and $^{\#\#\#}P < 0.001$ compared with the CPZ + Vehicle; $^{\&}P < 0.05$ compared with the CPZ + KMP. Data are mean ± SEM; number of animals per group = 6

MOG intensity in CPZ + KMP or CPZ + EXO-treated mice compared with the intact group (intact vs. CPZ + EXO = 0.0461, intact vs. CPZ + KMP = 0.0015). Compared with the CPZ + Vehicle treatment, treatment with EXOs ($P = 0.0224$) or the combination of EXO + KMP ($P = 0.0038$) led to an increase in MOG intensity. There was also a significant difference between the combination group and the KMP-administered group ($P = 0.0350$). (F (4, 10) = 16.01, $P = 0.0002$; Fig. 4D).

EXOs therapy in combination with KMP increased Myelin restoration in the cuprizone-demyelinated corpus callosum

In this study, the percentage of Black-Gold II staining intensity relative to that of the intact group was used as an index for evaluating the degree of myelination in the corpus callosum. Black-Gold II staining is a specific method for detecting myelin, where a decrease in staining intensity indicates demyelination and damage to the myelin sheath (Fig. 5A). The intensity ratio of the CPZ + Vehicle group to the intact group was significantly reduced compared to the CPZ + EXO ($P = 0.0005$) and CPZ + EXO + KMP groups ($P < 0.0001$). Furthermore, the intensity observed in the KMP group was significantly different from that in the co-administration group ($P = 0.0004$) and the CPZ + EXO group ($P = 0.0108$). (F (3, 8) = 38.75, $P < 0.0001$; Fig. 5B).

EXO and KMP combination therapy promotes oligodendrocyte gene expression and myelin repair in cuprizone-demyelinated mice

MBP gene expression was significantly greater in all the treatment groups than in the CPZ + Vehicle group (EXO: $P = 0.0018$, KMP: $P = 0.0081$, co-administration: $P < 0.0001$). In addition, *MBP* gene expression was greater in the CPZ + EXO + KMP group than in the CPZ + KMP and CPZ + EXO groups ($P < 0.0001$) (F (3, 20) = 33.57; Fig. 6A).

In addition, a significant increase in *Olig2* gene expression was observed only in the CPZ + EXO + KMP group compared with the CPZ + Vehicle group ($P = 0.0042$). However, there was no significant increase in *Olig2* gene expression in the CPZ + EXO + KMP group compared with the CPZ + EXO or CPZ + KMP groups (F (3, 20) = 5.553, $P = 0.0061$; Fig. 6B).

PDGFRα gene expression in the CPZ + EXO ($P = 0.0065$) and CPZ + EXO + KMP ($P = 0.0057$) groups was significantly lower than that in the CPZ + Vehicle group. Additionally, in the co-administered group ($P < 0.0001$), a greater reduction was found (F (3, 20) = 11.24, $P = 0.0002$; Fig. 6C).

EXO and KMP combination therapy enhances the Nrf2-driven antioxidant response in cuprizone-demyelinated mice

Nrf2 gene expression analysis revealed that the expression of this gene in the combined treatment group was significantly greater than that in the CPZ + Vehicle group (F (3, 20) = 13.19, $P < 0.0001$; Fig. 7A). A significant increase was also observed compared with the other two

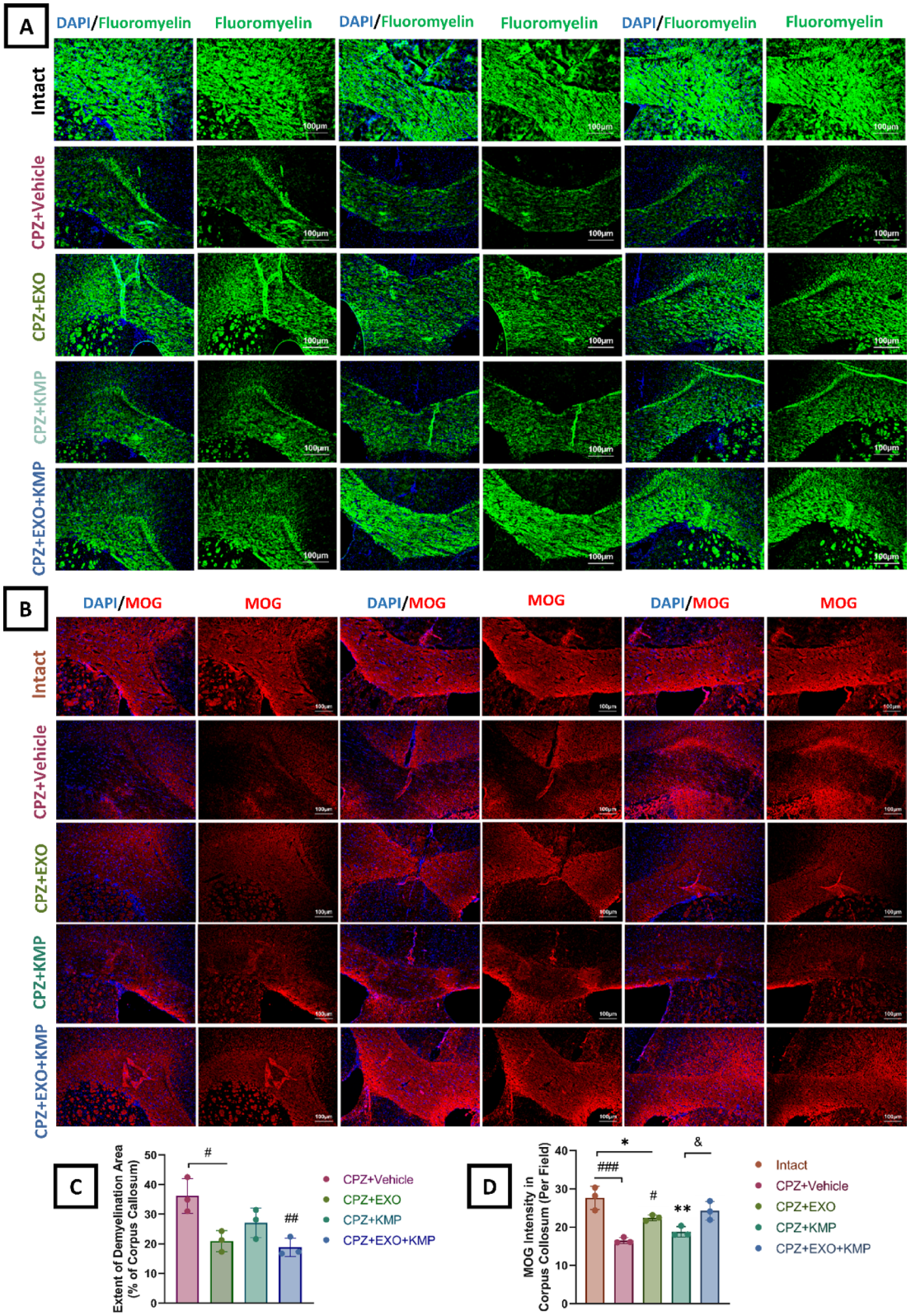

Fig. 4 (See legend on next page.)

(See figure on previous page.)

Fig. 4 FluoroMyelin and MOG staining in the corpus callosum of different groups after induction of demyelination via CPZ. **A** Representative FluoroMyelin staining (Green) and nuclear counterstaining (DAPI, blue) in the corpus callosum. Scale bar: 100 µm. **B** Immunostaining for MOG (red, myelin marker) in the corpus callosum, with nuclear counterstaining (DAPI, blue). Scale bar: 100 µm. **C** Quantitative analysis of the demyelinated area relative to the total corpus callosum area. Compared with the CPZ + Vehicle group, the CPZ + EXO group presented reduced demyelination. Compared with the CPZ + Vehicle group, the CPZ + EXO + KMP group presented a further significant reduction in demyelination. **D** Quantitative analysis of MOG immunointensity. Compared with the Intact group, the CPZ + Vehicle group presented significantly lower MOG expression. Compared with CPZ + Vehicle, treatment with EXOs or EXO + KMP restored MOG expression. Compared with the CPZ + KMP group, the CPZ + EXO + KMP group presented higher MOG intensity. Compared with the Intact group, the CPZ + EXO and CPZ + KMP groups presented reduced expression. $^{*}P < 0.05$ and $^{**}P < 0.01$ compared with the Intact; $^{\#}P < 0.05$, $^{\#\#}P < 0.01$, and $^{\#\#\#}P < 0.001$ compared with the CPZ + Vehicle; $^{\&}P < 0.05$ compared with CPZ + KMP. Data are mean ± SEM; number of samples per group: 3

treatments in which individual substances were administered (CPZ + EXO vs. CPZ + EXO + KMP: $P = 0.0008$; CPZ + KMP vs. CPZ + EXO + KMP: $P = 0.0122$).

HO-1 gene expression analysis revealed that the expression of this gene was significantly greater in the CPZ + EXO + KMP treatment group than in the CPZ + Vehicle group ($P = 0.0045$). (F (3, 20) = 5.322, $P = 0.0073$; Fig. 7B).

Nqo1 gene expression analysis revealed that the expression of this gene in the CPZ + EXO + KMP ($P = 0.0002$) and CPZ + EXO ($P = 0.0195$) treatment groups was significantly greater than that in the CPZ + Vehicle group (F (3, 20) = 9.759, $P = 0.0004$; Fig. 7C). In addition, compared with CPZ + KMP, the simultaneous use of EXO and KMP resulted in a greater increase in *Nqo1* gene expression ($P = 0.0255$).

EXO and KMP synergistically increased antioxidant activity and reduced lipid peroxidation profiling in cuprizone-demyelinated mice

Compared with the CPZ + Vehicle group, the intact group presented a greater level of TAC ($P < 0.0001$). There were also significant differences between the intact group and both the EXO-treated group ($P < 0.0001$) and the KMP-treated group ($P = 0.0217$). Additionally, the results of this test revealed that the TAC level in the EXO treatment and EXO + KMP simultaneous treatment groups was significantly greater ($P < 0.0001$) than that in the CPZ group. Compared with those in the EXO group, the groups in the KMP ($P = 0.0002$) and KMP + EXO ($P < 0.0001$) groups presented significant reductions (F (4, 25) = 41.64, $P < 0.0001$; Fig. 8A).

Lipid peroxidation was examined by measuring the level of MDA, an indicator of oxidative stress, in all the groups. The results obtained after statistical analysis revealed that the MDA levels in the EXO treatment ($P < 0.0001$), KMP treatment ($P < 0.0001$) and EXO + KMP simultaneous treatment ($P < 0.0001$) groups significantly decreased compared with those in the CPZ group (F (4, 25) = 85.43, $P < 0.0001$; Fig. 8B). The intact group also presented lower levels of MDA than did the CPZ group ($P < 0.0001$). There were also significant differences between the intact group and both the EXO treatment group ($P < 0.0001$) and the KMP-treated group ($P = 0.0011$).

The results of the statistical analyses revealed that the activity of the catalase enzyme in the CPZ group was significantly lower than that in the intact group ($P < 0.0001$). Additionally, the level of catalase in all the treatment groups significantly increased ($P < 0.0001$) compared with that in the CPZ group. However, a significant difference was still observed between the intact group and the KMP group ($P = 0.0021$), indicating that KMP alone also restored this parameter in the assay (F (4, 25) = 72.94, $P < 0.0001$; Fig. 8C).

The level of the SOD enzyme was examined as an indicator of antioxidant capacity in all the groups. The results revealed that the activity of this enzyme in the CPZ + Vehicle group ($P < 0.0001$) was significantly lower than that in the healthy control group. The levels of superoxide dismutase enzymes in the CPZ + EXO + KMP ($P = 0.0018$) and KMP groups ($P = 0.0042$) significantly increased. Despite the observed increase in activity within the EXO group, a significant difference was observed compared with that in the intact group ($P = 0.0276$), suggesting that EXO alone provided only partial improvement (F (4, 25) = 9.161, $P = 0.0001$; Fig. 8D).

The level of GPx, an indicator of antioxidant capacity, was examined in all the groups. The results revealed that the activity of this enzyme in the CPZ + Vehicle group was significantly lower ($P < 0.0001$) than that in the intact group (F (4, 25) = 54.18, $P < 0.0001$; Fig. 8E). In addition, the level of this enzyme in all the treatment groups was significantly greater than that in the CPZ + Vehicle group (KMP and KMP + EXO: $P < 0.0001$; EXO: $P = 0.0001$). On the other hand, significantly increased GPx activity was observed between the combined treatment group and the other two individually treated groups (CPZ + EXO vs. CPZ + EXO + KMP: $P < 0.0001$; CPZ + KMP vs. CPZ + EXO + KMP: $P = 0.0054$).

EXO and KMP combination therapy reduces glial activation in demyelinated corpus callosum

To investigate the effects of KMP and EXOs on microglial activity, the expression of Iba1, a microglial marker, was evaluated (Fig. 9A). The results revealed that the intensity of Iba1 in the corpus callosum of demyelinated mice treated with CPZ ($P < 0.0001$) was significantly greater than that in the corpus callosum of intact mice (F

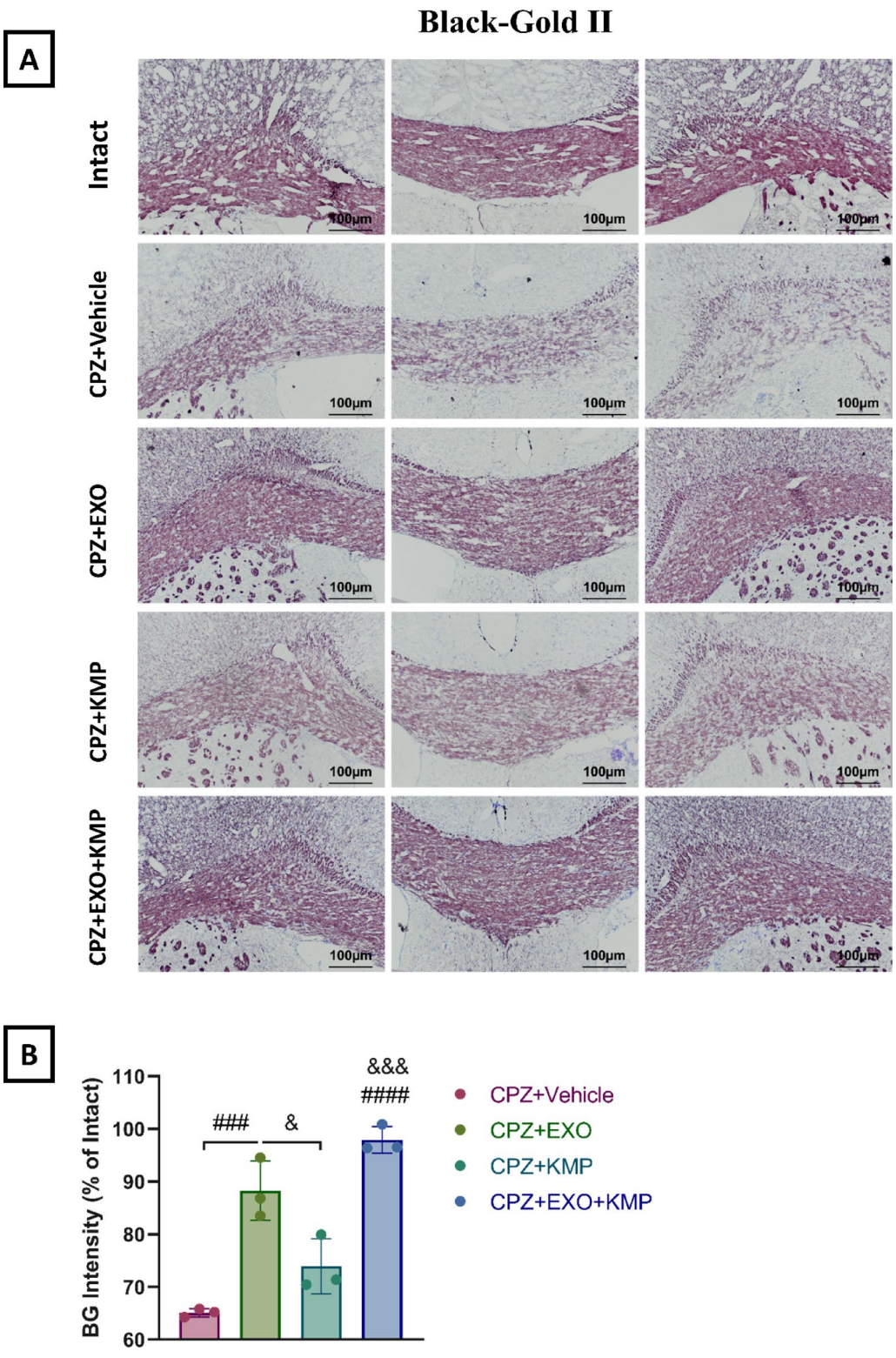

Fig. 5 EXO monotherapy combined with KMP enhances myelin restoration in the CPZ-demyelinated corpus callosum. **A** Representative Black-Gold II staining of myelin in the corpus callosum; decreased staining intensity indicates demyelination. Scale bar: 100 µm. **B** Quantitative analysis of B&G staining intensity (myelination index). Compared with the CPZ + Vehicle group, the CPZ + EXO and CPZ + EXO + KMP groups presented restored myelination. $^{###}P < 0.001$ and $^{####}P < 0.0001$ compared with the CPZ + Vehicle; $^{\&}P < 0.05$ and $^{\&\&\&}P < 0.001$ with the CPZ + KMP. Data are mean ± SEM; number of samples per group: 3

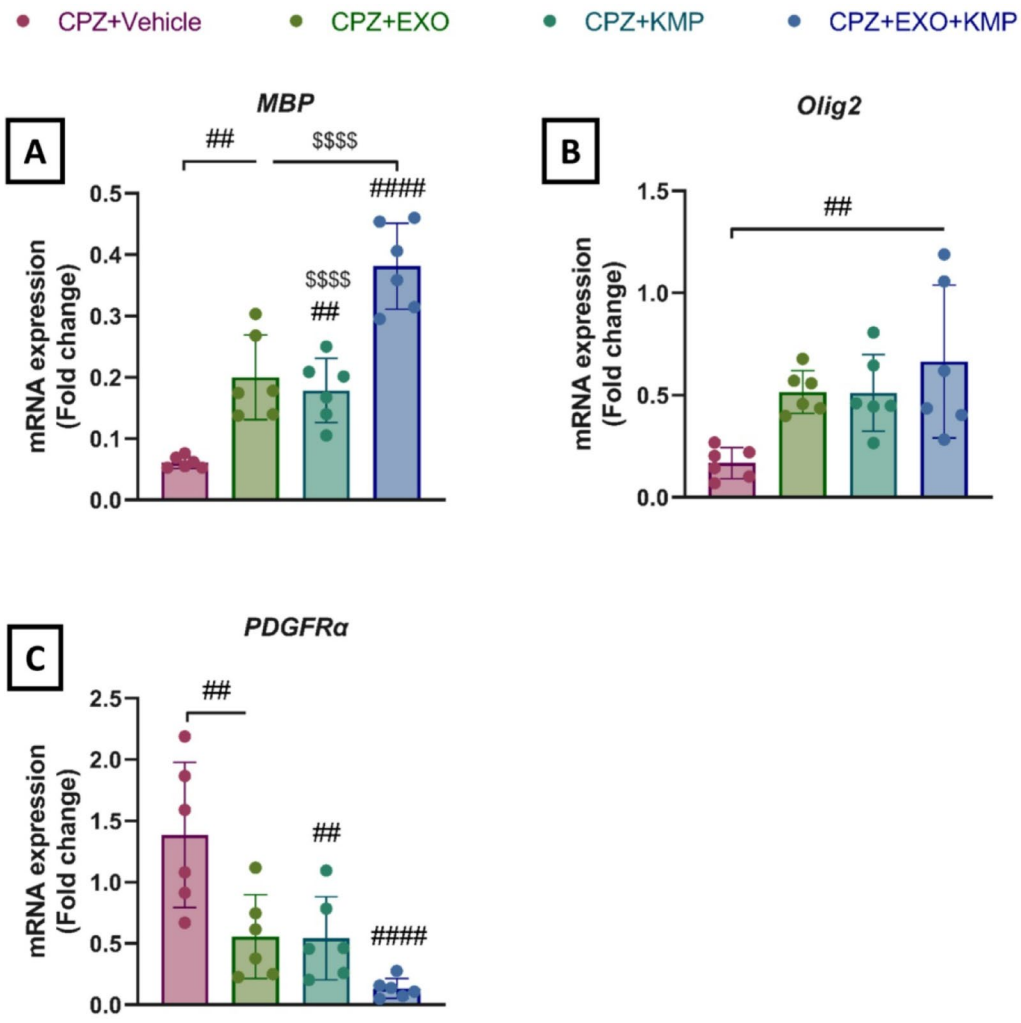

Fig. 6 Effect of EXO and KMP combination therapy on oligodendrocyte gene expression in CPZ-demyelinated mice. **A***MBP* expression levels. Compared with the CPZ + Vehicle group, all the treatment groups presented elevated *MBP* expression. **B***Olig2* expression levels. Compared with the CPZ + Vehicle group, only the CPZ + EXO + KMP group presented increased expression. **C***PDGFRα* expression levels. Compared with the CPZ + Vehicle group, the CPZ + EXO and CPZ + KMP groups presented reduced expression. Compared with the CPZ + Vehicle group, the CPZ + EXO + KMP group presented a further significant reduction. Gene expression was normalized via the $2^{-\Delta\Delta CT}$ method relative to *Eef2*. $^{\#\#}P < 0.01$ and $^{\#\#\#\#}P < 0.0001$ compared with the CPZ + Vehicle; $P < 0.0001$ compared with the CPZ + EXO + KMP. Data are mean ± SEM; number of animals per group: 6

(4, 10) = 30.83, $P < 0.0001$; Fig. 9C). Compared with the CPZ group, the EXO ($P = 0.2087$) and KMP ($P = 0.9989$) groups did not exhibit reduced expression of this marker. However, compared with KMP treatment alone, the combination of KMP and EXO significantly reduced the intensity of Iba1 positive cells ($P = 0.0019$). Significant differences were also observed between the intact group and all treated groups (EXO: $P = 0.0004$, KMP; $P < 0.0001$, EXO + KMP: $P = 0.0370$; Fig. 9C).

To investigate the effects of KMP and EXOs on astrocyte activity, the expression of GFAP, an astrocyte marker, was evaluated (Fig. 9B). The results revealed that the number of GFAP-expressing cells in the corpus callosum of CPZ-demyelinated mice was significantly greater than that in the corpus callosum of intact mice ($P = 0.0016$). On the other hand, the EXO group ($P = 0.0247$) and EXO + KMP group ($P = 0.0066$) exhibited significant decreases in expression compared with the CPZ + Vehicle group (Fig. 9D). Despite the decrease in the intensity of GFAP$^+$ cells in the KMP group, there was no significant difference compared with that in the CPZ + Vehicle group ($P = 0.2381$), but a significant difference was found compared with that in the intact group (intact vs. CPZ + KMP: $P = 0.0454$). These findings suggest the anti-inflammatory potential of EXOs and co-administration of EXOs and KMP (F (4, 10) = 9.614, $P = 0.0019$).

Combined EXO and KMP therapy reduces pro-inflammatory cytokine expression in demyelinated mice

IL-1β gene expression was significantly lower in all treatment groups (all groups $P < 0.0001$) than in the

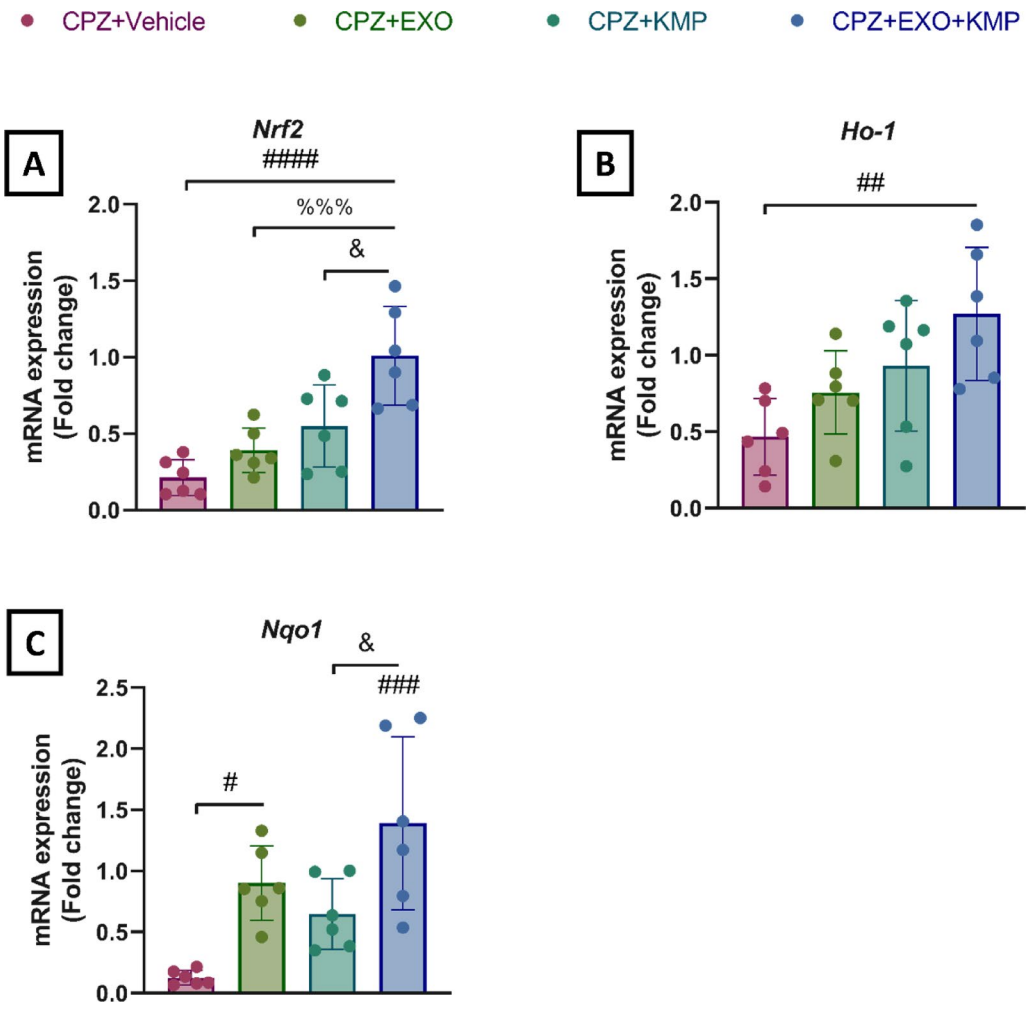

Fig. 7 Effect of EXO and KMP combination therapy on Nrf2-driven antioxidant gene expression in cuprizone-demyelinated mice. **A***Nrf2* expression levels. Compared with the CPZ + Vehicle group, the CPZ + EXO + KMP, CPZ + EXO, and CPZ + KMP groups presented significantly increased expression. **B***HO-1* expression levels. Compared with the CPZ + Vehicle group, the CPZ + EXO + KMP group presented elevated expression of these genes. **C***Nqo1* expression levels. Compared with the CPZ + Vehicle group, the CPZ + EXO + KMP and the CPZ + EXO groups presented increased expression. Compared with CPZ + KMP, CPZ + EXO + KMP also resulted in greater expression. Gene expression was normalized via the $2^{-\Delta\Delta CT}$ method relative to *Eef2*. $^{\#}P < 0.05$, $^{\#\#}P < 0.01$, $^{\#\#\#}P < 0.001$, and $^{\#\#\#\#}P < 0.0001$, compared with the CPZ + Vehicle; $^{\&}P < 0.05$ compared with the CPZ + KMP; $^{\%\%\%}P < 0.001$ compared with the CPZ + EXO. Data are mean ± SEM; number of animals per group: 6

CPZ + Vehicle group ($F(3, 20) = 19.40$, $P < 0.0001$; Fig. 10A).

In addition, *IL-18* gene expression analysis revealed that the expression of this gene was significantly lower in all treatment groups (EXO: $P < 0.0001$, KMP: $P = 0.0002$, combination: $P < 0.0001$) than in the CPZ + Vehicle group ($F(3, 20) = 16.62$, $P < 0.0001$; Fig. 10B).

TNF-α gene expression was significantly lower in all the treatment groups than in the CPZ + Vehicle group ($F(3, 20) = 15.49$, $P < 0.0001$; Fig. 10C), and this reduction was greater in the combination group ($P < 0.0001$) than in the other two groups (EXO: $P = 0.0002$, KMP: $P = 0.0087$).

Discussion

A multifaceted approach is a major part of the development of new treatments for inflammatory, oxidative, and degenerative neurological disorders with complex pathologies, including MS [30]. Therefore, combination therapeutics targeting pathological processes such as both the inflammation and oxidative stress pathways are potential strategies for mitigating MS. While current therapies primarily address inflammation [31], oxidative stress remains an unnoticed target. Hence, the combination of MSC-derived EXOs with anti-inflammatory agents [32], with KMP serving as an antioxidant [33], in a CPZ-induced demyelination model could reduce neuroinflammation and oxidative stress, which leads to enhanced remyelination and functional recovery,

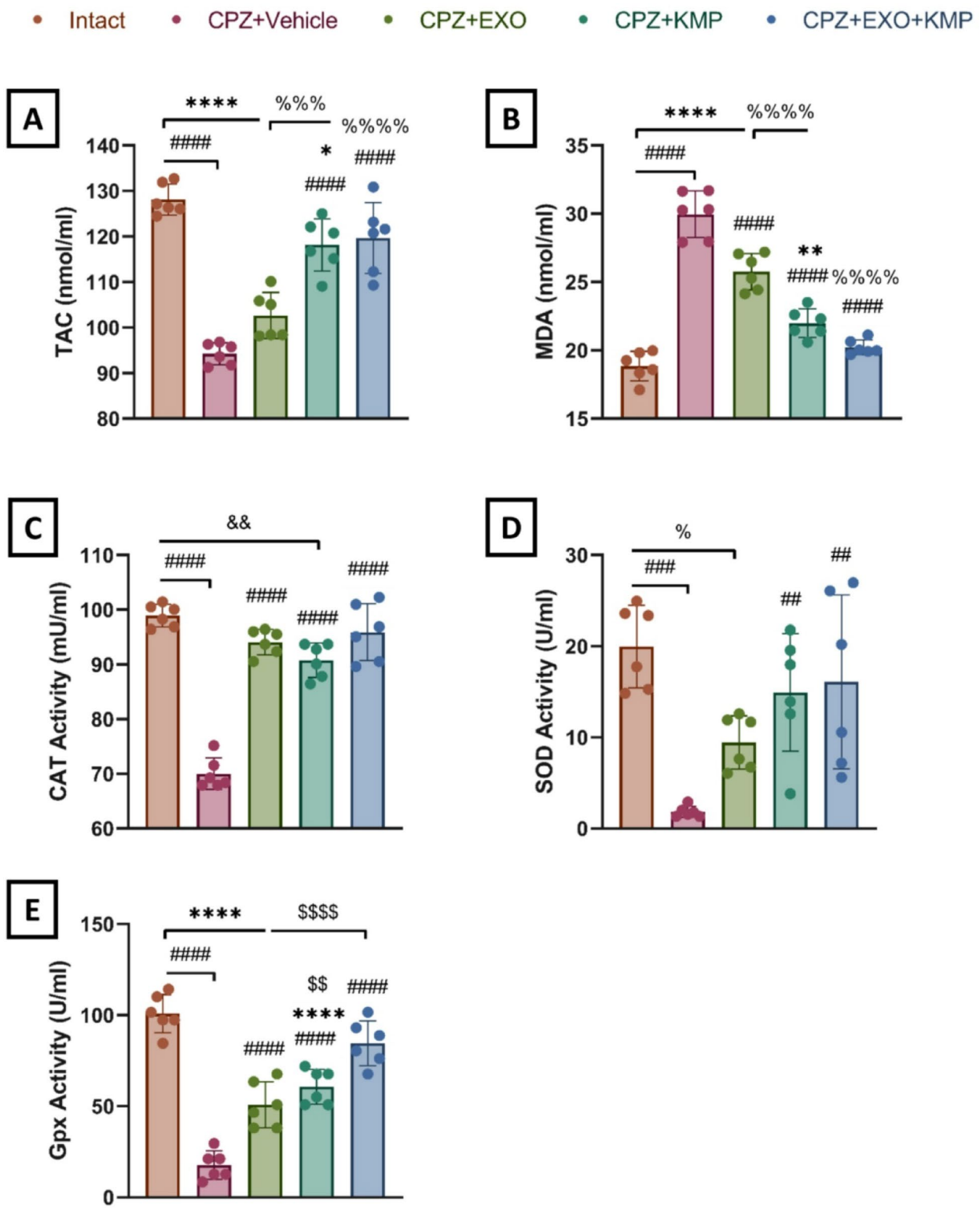

Fig. 8 EXO and KMP combination therapy enhances antioxidant activity and reduces lipid peroxidation in cuprizone-demyelinated mice. **A** Total antioxidant capacity (TAC) decreased in CPZ + Vehicle and increased in CPZ + KMP and CPZ + EXO + KMP. **B** Malondialdehyde (MDA) levels increased in CPZ + Vehicle and decreased in all treatment groups. **C** Catalase activity decreased in CPZ + Vehicle and increased in all treatment groups. **D** Superoxide dismutase (SOD) activity decreased in CPZ + Vehicle and increased in CPZ + KMP and CPZ + EXO + KMP. **E** Glutathione peroxidase (GPx) activity increased in all treatment groups. $^{*}P < 0.05$, $^{**}P < 0.01$, and $^{****}P < 0.0001$ compared with the Intact; $^{\#\#}P < 0.01$, $^{\#\#\#}P < 0.001$, and $^{\#\#\#\#}P < 0.0001$ compared with the CPZ + Vehicle; $^{\%}P < 0.05$, $^{\%\%\%}P < 0.001$, and $^{\%\%\%\%}P < 0.0001$ compared with the CPZ + EXO; $^{\&\&}P < 0.01$ and $^{\&\&\&}P < 0.001$, compared with CPZ + KMP; $^{\$\$}P < 0.01$ and $P < 0.0001$ compared with CPZ + EXO + KMP. Data are mean ± SEM; $n = 6$ per group

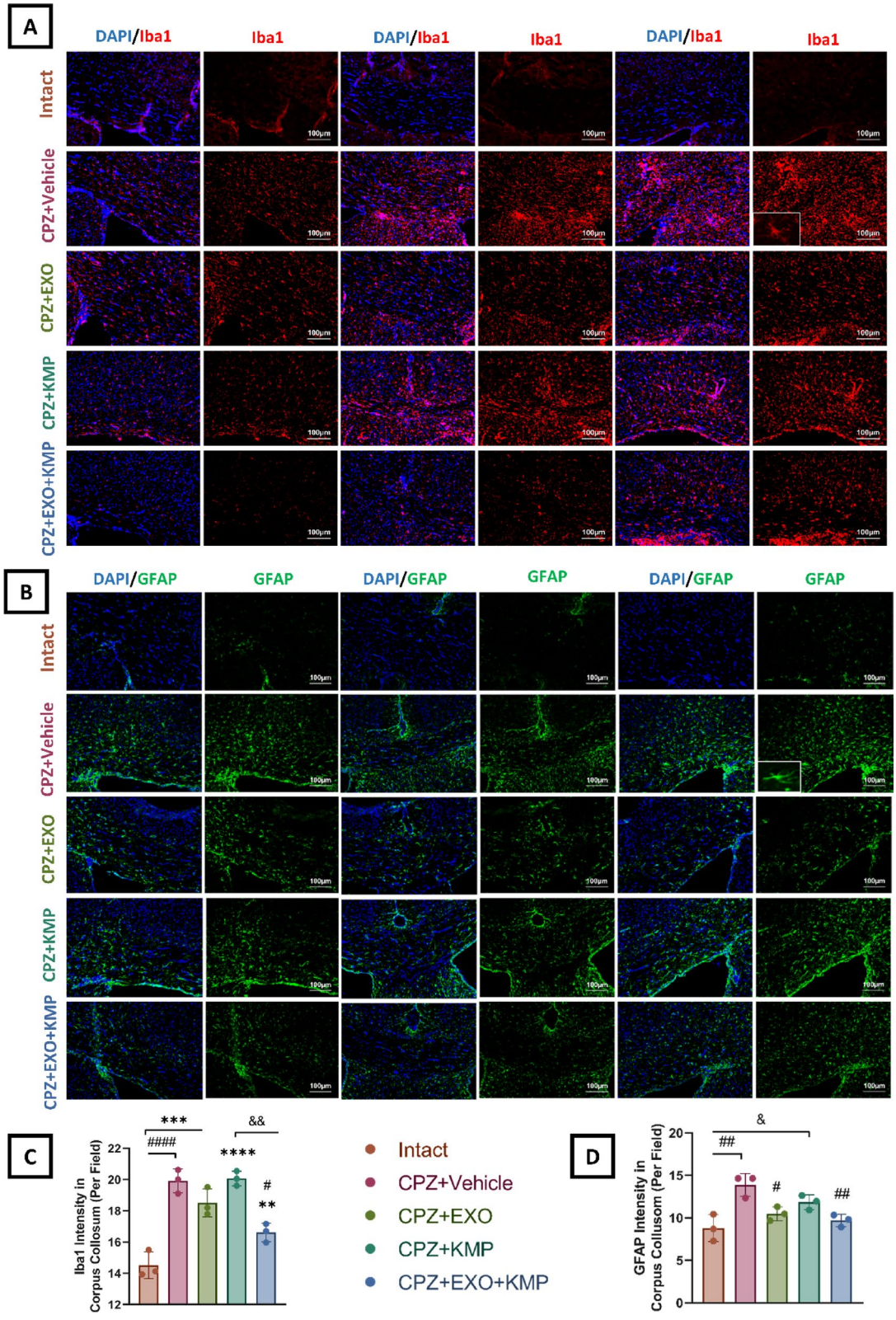

Fig. 9 Effect of EXO and KMP on astrocyte activity and microglial activation in the demyelinated corpus callosum. **A** Immunofluorescence staining for Iba1. Scale bar: 100 μm. **B** Immunofluorescence staining for GFAP. Scale bar: 100 μm. **C** Quantification of Iba1 intensity. **D** Quantification of GFAP intensity. Data are mean ± SEM; $n = 3$ per group. $^{**}P < 0.01$, $^{***}P < 0.001$, and $^{****}P < 0.0001$ compared with the Intact group; $^{\#}P < 0.05$ and $^{\#\#}P < 0.01$, and $^{\#\#\#\#}P < 0.0001$ compared with the CPZ + Vehicle; $^{\&}P < 0.05$ and $^{\&\&}P < 0.05$ compared to the CPZ + KMP. Data are mean ± SEM; number of animals per group: 3

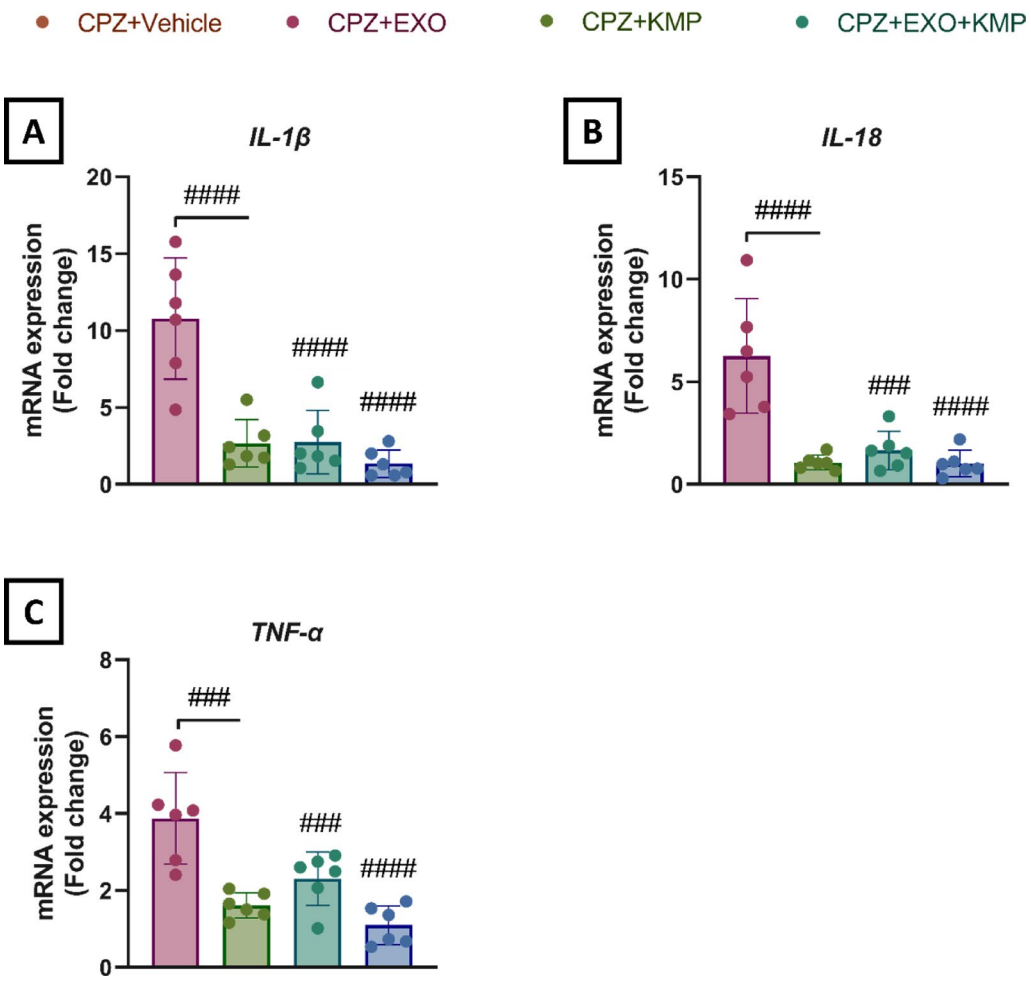

Fig. 10 Impact of EXO and KMP combination therapy on pro-inflammatory cytokine expression in cuprizone-demyelinated mice. **A***IL-1β* gene expression levels. Compared with CPZ + Vehicle, all the other treatments significantly reduced IL-1β expression. **B***IL-18* gene expression levels. Compared with the CPZ + Vehicle group, all the treatment groups presented reduced *IL-18* expression. **C***TNF-α* gene expression levels. *TNF-α* expression decreased in all the treatment groups compared with that in the CPZ + Vehicle group. $^{###}P < 0.001$ and $^{####}P < 0.0001$ compared with the CPZ + Vehicle. Data are mean ± SEM; number of animals per group: 6

followed by neuroprotection. In our study, we observed the multifaceted advantages of combination therapy in four major sections, including behavioral, histological, molecular, and biochemical parameters.

In the present study, ICV administration of KMP was designed to deliver this substance directly into the brain, which ensures its localized antioxidant effects and, therefore, maximum bioavailability without existing issues regarding BBB permeability. It also allows for easier assessment of its potential within the CNS. Additionally, EXOs were administered intranasally to facilitate their ability to target the brain rather than depending on their natural ability to cross the BBB. This potential makes them ideal for delivering anti-inflammatory markers such as various cytokines and miRNAs across the BBB to regulate the immune response [34]. Furthermore, combining these agents was hypothesized to target both key pathological pathways mentioned at the same time, leading to synergistic neuroprotection and remyelination such that neither of these monotherapies could provide the same efficiency individually.

In the present study, we assessed behavioral parameters through Y-Maze, NADT and Wire hang to test the combination of EXO and KMP to evaluate their efficacy. Compared with the individual therapies, the combination treatment significantly improved spontaneous alternation percentages in the Y-maze test, which indicated more efficient working memory [35]. However, a lesser effect was observed in the novel arm test, which could be due to the different sensitivities of these experiments to other related cognitive aspects of the mice. The Y-maze is considered to capture even small improvements in cognition more effectively than the novel arm test does [36]. Another study revealed that EXOs derived from MSCs mitigate cognitive impairment in Alzheimer's disease (AD)-like mice via the Y-maze test by improving

brain-derived neurotrophic factor (BDNF)-related neuropathology [37]. Similarly, the results of another study revealed that KMP treatment improved learning and memory ability through the Y-maze test [38]. Additionally, the Wire Hang test was used to assess motor function, grip strength, and neuromuscular junction health [39], which also exhibited promising results with the EXO + KMP combination. There were slight variations between the reach score parameter and hanging duration, which might be due to the local impact of ICV cannulation in stereotaxic surgery on mice rather than a true reflection of motor capability, alongside the possibility of limited KMP diffusion when not injected systemically in the present study [38]. In another study, treatment with miR-188-3p-overexpressing EXOs increased the hanging time, indicating that neuromuscular strength was significantly improved [40]. The hanging wire test in another study revealed that after 2 weeks of KMP treatment, the number of falls was lower than that in the control [41].

Changes in motor behavior are the direct consequence of damaging mechanisms responsible for demyelination. Thus, we used multiple myelination markers, such as FluoroMyelin, Black-Gold II, and MOG, to comprehensively evaluate different aspects of myelin integrity and repair procedures, from structural to functional recovery of oligodendrocyte populations [42, 43]. EXO + KMP treatment reduced demyelination, as evidenced by the presence of FluoroMyelin and Black-Gold II, which was associated with increased expression of myelin-related genes (MBPs) and markers (MOGs). On the other hand, the decreased expression levels of PDGFRα suggest a reduction in reactive OPCs, which was confirmed by improved oligodendrocyte gene profiles (Olig2). Other studies have assessed morphological changes in brain tissues through diverse protocols with similar findings. One study performed MBP immunofluorescence staining and revealed that the corpus callosum area in the BM-MSC-treated group was greater than that in the chronic CPZ-induced demyelination group. Additionally, relatively more myelinated nerve fibers in the corpus callosum were observed via TEM [44].

Demyelination-remyelination processes are closely related to the increase/decrease in the activities of enzymes involved in oxidative stress and the remaining metabolites. The up regulation of key antioxidant markers, including *Nrf2*, *HO-1*, and *NQO1*, indicates the activation of the brain's innate immunity against oxidative stress [45]. Nrf2, as a central regulatory mediator, is activated and subsequently moves into the nucleus and triggers the transcription of multiple genes involved in neuroprotection, including HO-1 and NQO1. These genes are essential for decreasing reactive oxygen species (ROS) levels within cells [46]. This biological reaction is facilitated by antioxidant biochemical markers, such as elevated TAC and increased activation of antioxidant enzymes, including SOD, CAT, and GPx. Furthermore, a decrease in the level of MDA, a primary metabolite of lipid peroxidation, eventually reduces oxidative damage [47]. Our dual therapeutic approach up regulated the expression of antioxidant markers and improved the antioxidant profiles described previously. Another study revealed a reduction in MDA and an increase in SOD activity after MSC transplantation [48]. On the other hand, another study confirmed that KMP is a potent inhibitor of Nrf2 by assessing target genes such as HO-1 and NQO1, similar to our study [49]. KMP has also been investigated for its anti-apoptic and therefore anticancer properties. It was concluded that this substance reduces cancer cell proliferation and induces apoptosis in non-small cell lung cancer (NSCLC) cells by inhibiting the Nrf2 signaling pathway [49].

Finally, we examined the differences in the expression of pro-inflammatory elements that are closely involved in disease progression and can act as mediators of both demyelination and oxidative stress mechanisms. EXO + KMP administration significantly reduced neuroinflammation, as evidenced by the reduced activation of astrocytes and microglia. Our immunofluorescence studies revealed lower levels of GFAP and Iba1 expression, suggesting suppressed glial reactivity in brain tissues [50]. This reduced cell activity was followed by notable decreases in the expression levels of pro-inflammatory cytokine genes, which are involved in neuroinflammatory pathways and lead to neural injury [51]. Moreover, in another study, combination therapy involving MSC transplantation with L-a-aminoadipate caused a significant decrease in the number of GFAP+ and Iba-1+ cells compared with that in CPZ-treated mice [52]. To further explore the potential of KMP, another study performed Iba-1 staining in cerebral ischemia/reperfusion rats and reported that the number and size of activated microglia decreased in a dose-dependent manner [53]. Together, these results suggest that treatment not only impacts inflammatory cell activities but also interferes with molecular pathways involved in inflammation, creating conditions to achieve neuroprotection that could promote remyelination and neurological repair.

Noteworthy, the therapeutic actions of MSC-derived EXOs observed in our study are likely mediated by known bioactive cargo, including miRNAs such as miR-219 that have been shown to stimulate OPC differentiation and remyelination [54], regulation of antioxidant pathways such as the Nrf2/HO-1 axis by MSC-EXOs [55], and also transportation of immunomodulatory proteins and cytokines (such as IL-10 and TGF-β) and neurotrophic factors that reduce glial activation plus inflammatory cytokine expression, supporting survival and maturation of oligodendrocytes [56]. Although we

did not characterize the specific miRNA or protein content of the EXOs used here, these previous data provide a mechanistic framework for the reductions in inflammation, increases in antioxidant markers, up regulation of myelin genes, and functional improvements observed with EXO + KMP therapy.

Our study resulted in the combination of KMP + EXO showing a strong potential when administered via i.c.v and i.n, respectively. The rationale for using i.c.v delivery of KMP in this experimental design was to bypass the BBB and directly assess its antioxidant efficacy within the CNS, thereby maximizing bioavailability and minimizing confounding factors related to systemic metabolism. However, KMP administration is thought to cause possible stress induction due to its invasive feature and it is considered to be far from a probable clinical-friendly strategy. For translational relevance, it is important to consider less invasive candidates. Several studies have reported that intranasal administration can effectively deliver small molecules and nanoparticles into the brain, offering a practical route that bypasses the BBB [57, 58]. Intragastric infusion and intraperitoneal injection of KMP and related flavonoids have also been shown to exert neuroprotective and antioxidant effects, though bioavailability is influenced by metabolism, absorption, and dosing strategy [59, 60]. Thus, more studies are needed to completely evaluate the best efficacy of our target combination considering both different optimal dosage and also the administration routes (e.g. i.p., i.g. etc.). Additionally, our study suggests future investigations to re-design their methodology in the context of more extended treatment timeline to achieve better vision of this duo's involved mechanisms and potential therapeutic future.

Conclusion

The present study demonstrated that dual-targeted therapy combining MSC-derived EXOs and KMP potentially impacts on remyelination and cognitive functions in a CPZ-induced demyelination model. The mentioned mechanisms involved to inhibit oxidative stress and neuroinflammation, also highlights two main pathological mechanisms in MS. Our findings suggest further investigations regarding optimized delivery systems and extended studies, with the goal of examining this methodology into effective possible clinical strategies for demyelinating disorders such as MS.

Abbreviations

AD	Alzheimer's disease
ANOVA	Analysis of variance
BBB	Blood–brain barrier
BCA	Bicinchoninic acid
BDNF	Brain-derived neurotrophic factor
CAT	Catalase
CNS	Central nervous system
DMEM/F12	Dulbecco's modified Eagle's medium/nutrient mixture F-12
DLS	Dynamic light scattering
EXO	Exosomes
FBS	Fetal bovine serum
GPx	Glutathione peroxidase
ICV	Intracerebroventricular
MDA	Malondialdehyde
MSC	Mesenchymal stem cell
MOG	Myelin oligodendrocyte glycoprotein
NTA	Nanoparticle tracking analysis
NADT	Novel arm discrimination test
NSCLC	Non-small cell lung cancer
PFA	Paraformaldehyde
P/S	penicillin/streptomycin
PBS	Phosphate-buffered saline
qRT-PCR	Quantitative real-time PCR
ROS	Reactive oxygen species
SOD	Superoxide dismutase
TAC	Total antioxidant capacity
TEM	Transmission electron microscopy

Acknowledgements

The authors declare that they have not used AI-generated work in this manuscript. The schematic figure and graphical abstract were created with BioRender.com.

Author contributions

Conceptualization: F.R., H.A., and M.G.; Methodology: F.R., H.A., C.L., G.L., R.P., G.B. and M.G.; Software: F.R. and H.A.; Validation: F.R., H.A., G.B. and M.G.; Formal analysis: F.A., H.A. and M.G.; Data curation: F.R., H.A., G.B. and M.G.; Writing original draft preparation: F.A.; Writing-review and editing: M.G. and G.B.; Visualization: M.G.; Supervision: G.B. and M.G.; Project administration: M.G. All authors have seen and approved the final version of the manuscript being submitted. They warrant that the article is the authors' original work, hasn't received prior publication and isn't under consideration for publication elsewhere.

Funding

This research was financially supported by the Iran National Science Foundation (INSF) (Grant No. 4028282) and Babol University of Medical Sciences (Grant No: 724135444) and was performed as part of General Medicine thesis.

Data availability

The data will be made available upon request.

Declarations

Ethics approval and consent to participate

All procedures were approved by the Ethics Committee of Babol University of Medical Sciences (IR.MUBABOL.AEC.1402.019) and adhered to the NIH Guide for the Care and Use of Laboratory Animals and ARRIVE guidelines. This project entitled "Investigating the effect of simultaneous administration of kaempferol and exosome derived from mouse bone marrow mesenchymal stem cells on myelin repair of corpus callosum in cuprizone-induced demyelination model" was approved on February 13, 2024.

Consent for publication

Not applicable.

Competing interests

The authors declare no competing interests.

Received: 8 June 2025 / Accepted: 9 October 2025
Published online: 03 November 2025

References

1. Bjartmar C, Trapp BD. Axonal and neuronal degeneration in multiple sclerosis: mechanisms and functional consequences. Curr Opin Neurol. 2001;14(3):271–8.
2. Pegoretti V, Swanson KA, Bethea JR, Probert L, Eisel ULM, Fischer R. Inflammation and oxidative stress in multiple sclerosis: consequences for therapy development. Oxid Med Cell Longev. 2020;2020:7191080.
3. Travers P, Walport M, Shlomchik MJ, Janeway M. Immunobiology: the immune system in health and disease. Churchill Livingstone New York, NY, USA; 1997.
4. Zaman M, Huissoon A, Buckland M, Patel S, Alachkar H, Edgar JD, et al. Clinical and laboratory features of seventy-eight UK patients with good's syndrome (thymoma and hypogammaglobulinaemia). Clin Exp Immunol. 2019;195(1):132–8.
5. Azizi G, Yazdani R, Rae W, Abolhassani H, Rojas M, Aghamohammadi A, et al. Monogenic polyautoimmunity in primary immunodeficiency diseases. Autoimmun Rev. 2018;17(10):1028–39.
6. Milo R, Panitch H. Combination therapy in multiple sclerosis. J Neuroimmunol. 2011;231(1):23–31.
7. Mashouri L, Yousefi H, Aref AR, Ahadi Am, Molaei F, Alahari SK. Exosomes: composition, biogenesis, and mechanisms in cancer metastasis and drug resistance. Mol Cancer. 2019;18:1–14.
8. Qiu Y, Luo Y, Guo G, Meng J, Bao N, Jiang H. BMSCs-derived exosomes carrying miR-668-3p promote progression of osteoblasts in osteonecrosis of the femoral head: expression of proteins CD63 and CD9. Int J Biol Macromol. 2024;280:136177.
9. Zonouz AM, Rahbardar MG, Alibolandi M. Exosome-based platforms for treatment of multiple sclerosis. Brain Res Bull. 2025;222:111256.
10. Gangadaran P, Madhyastha H, Madhyastha R, Rajendran RL, Nakajima Y, Watanabe N, et al. The emerging role of exosomes in innate immunity, diagnosis and therapy. Front Immunol. 2022;13:1085057.
11. Mycko MP, Baranzini SE. MicroRNA and exosome profiling in multiple sclerosis. Mult Scler. 2020;26(5):599–604.
12. Kim E, Cui J, Zhang G, Lee Y. Physiological effects of Green-Colored Food-Derived bioactive compounds on cardiovascular and metabolic diseases. Appl Sci. 2022;12(4):1879.
13. Calderón-Montaño JM, Burgos-Morón E, Pérez-Guerrero C, López-Lázaro M. A review on the dietary flavonoid Kaempferol. Mini Rev Med Chem. 2011;11(4):298–344.
14. Wang J, Fang X, Ge L, Cao F, Zhao L, Wang Z, et al. Antitumor, antioxidant and anti-inflammatory activities of Kaempferol and its corresponding glycosides and the enzymatic Preparation of Kaempferol. PLoS ONE. 2018;13(5):e0197563.
15. Silva dos Santos J, Goncalves Cirino JP, de Oliveira Carvalho P, Ortega MM. The Pharmacological action of Kaempferol in central nervous system diseases: a review. Front Pharmacol. 2021;11:565700.
16. Kashyap D, Sharma A, Tuli HS, Sak K, Punia S, Mukherjee TK. Kaempferol–A dietary anticancer molecule with multiple mechanisms of action: recent trends and advancements. J Funct Foods. 2017;30:203–19.
17. Wang F, Wang L, Qu C, Chen L, Geng Y, Cheng C, et al. Kaempferol induces ROS-dependent apoptosis in pancreatic cancer cells via TGM2-mediated Akt/mTOR signaling. BMC Cancer. 2021;21:1–11.
18. Askari H, Yavarpour-Bali H, Shirzad M, Sadeghi F, Biagini G, Ghasemi-Kasman M. Combination therapy with exosomes and NLRP3 Inhibition enhances Myelin repair in a cuprizone-induced demyelination model. Eur J Pharmacol. 2025;1002:177851.
19. Zhdanova DY, Poltavtseva RA, Svirshchevskaya EV, Bobkova NV. Effect of intranasal administration of multipotent mesenchymal stromal cell exosomes on memory of mice in alzheimer's disease model. Bull Exp Biol Med. 2021;170(4):575–82.
20. Suzuki K, Kikkawa Y. Status spongiosus of CNS and hepatic changes induced by Cuprizone (biscyclohexanone oxalyldihydrazone). Am J Pathol. 1969;54(2):307–25.
21. Riazifar M, Mohammadi MR, Pone EJ, Yeri A, Lässer C, Segaliny AI, et al. Stem Cell-Derived exosomes as nanotherapeutics for autoimmune and neurodegenerative disorders. ACS Nano. 2019;13(6):6670–88.
22. Kalaki-Jouybari F, Shirzad M, Javan M, Ghasemi-Kasman M, Pouramir M. Co-administration of naringin and NLRP3 inhibitor improves Myelin repair and mitigates oxidative stress in Cuprizone-Induced demyelination model. Curr Neuropharmacol. 2025;23(4):475–91.
23. Kraeuter AK, Guest PC, Sarnyai Z. The Y-Maze for assessment of Spatial working and reference memory in mice. Methods Mol Biol. 2019;1916:105–11.
24. Noor BK, Mansouri R, Alsufiani H, Alghamdi B. Investigation of the optimal dose for experimental lipopolysaccharide-induced recognition memory impairment: behavioral and histological studies. J Integr Neurosci. 2022;21:49.
25. Anjomani Virmouni S, Ezzatizadeh V, Sandi C, Sandi M, Al-Mahdawi S, Chutake Y, et al. A novel GAA repeat expansion-based mouse model of Friedreich ataxia. Dis Models Mech. 2015;8:225–35.
26. Ghasemi-Kasman M, Shojaei A, Gol M, Moghadamnia AA, Baharvand H, Javan M. miR-302/367-induced neurons reduce behavioral impairment in an experimental model of alzheimer's disease. Mol Cell Neurosci. 2018;86:50–7.
27. He J, Wang Y, Zhao ZH, He JY, Gao MY, Wang JQ, et al. Exosome-specific loading Sox10 for the treatment of Cuprizone-induced demyelinating model. Biomed Pharmacother. 2024;171:116128.
28. Naeimi R, Baradaran S, Ashrafpour M, Moghadamnia AA, Ghasemi-Kasman M. Querectin improves Myelin repair of optic Chiasm in lyolecithin-induced focal demyelination model. Biomed Pharmacother. 2018;101:485–93.
29. Schmued L, Bowyer J, Cozart M, Heard D, Binienda Z, Paule M. Introducing Black-Gold II, a highly soluble gold phosphate complex with several unique advantages for the histochemical localization of Myelin. Brain Res. 2008;1229:210–7.
30. Dash UC, Bhol NK, Swain SK, Samal RR, Nayak PK, Raina V, et al. Oxidative stress and inflammation in the pathogenesis of neurological disorders: mechanisms and implications. Acta Pharm Sinica B. 2025;15(1):15–34.
31. Haase S, Linker RA. Inflammation in multiple sclerosis. Ther Adv Neurol Disord. 2021;14:17562864211007687.
32. Shen Z, Huang W, Liu J, Tian J, Wang S, Rui K. Effects of mesenchymal stem Cell-Derived exosomes on autoimmune diseases. Front Immunol. 2021;12:749192.
33. Sharma N, Biswas S, Al-Dayan N, Alhegaili AS, Sarwat M. Antioxidant role of Kaempferol in prevention of hepatocellular carcinoma. Antioxid (Basel). 2021;10(9):1419.
34. Li C, Qin S, Wen Y, Zhao W, Huang Y, Liu J. Overcoming the blood-brain barrier: exosomes as theranostic nanocarriers for precision neuroimaging. J Controlled Release. 2022;349:902–16.
35. Melbiarta R, Kalanjati V, Herawati L, Salim Y, Othman Z. Analysis of Spatial working memory using the Y-Maze on rodents treated with High-Calorie diet and Moderate-Intensity exercise. Folia Med Indonesiana. 2022;59:40–5.
36. d'Isa R, Comi G, Leocani L. Apparatus design and behavioural testing protocol for the evaluation of Spatial working memory in mice through the spontaneous alternation T-maze. Sci Rep. 2021;11(1):21177.
37. Liu S, Fan M, Xu JX, Yang LJ, Qi CC, Xia QR, et al. Exosomes derived from bone-marrow mesenchymal stem cells alleviate cognitive decline in AD-like mice by improving BDNF-related neuropathology. J Neuroinflammation. 2022;19(1):35.
38. Wang M, Xia Y, Ai S, Gu X, Wang HL. Kaempferol improves Pb-induced cognitive impairments via inhibiting autophagy. J Nutr Biochem. 2024;125:109556.
39. Mettlach G, Polo-Parada L, Peca L, Rubin CT, Plattner F, Bibb JA. Enhancement of neuromuscular dynamics and strength behavior using extremely low magnitude mechanical signals in mice. J Biomech. 2014;47(1):162–7.
40. Li Q, Wang Z, Xing H, Wang Y, Guo Y. Exosomes derived from miR-188-3p-modified adipose-derived mesenchymal stem cells protect parkinson's disease. Mol Ther Nucleic Acids. 2021;23:1334–44.
41. Pilotto F, Smeele P, Scheidegger O, Diab R, Schobesberger M, Sierra-Delgado A, et al. Kaempferol enhances ER-mitochondria coupling and protects motor neurons from mitochondrial dysfunction and ER stress in C9ORF72-ALS. Acta Neuropathol Commun. 2025;13:21.
42. Simons M, Nave KA, Oligodendrocytes. Myelination and axonal support. Cold Spring Harb Perspect Biol. 2015;8(1):a020479.
43. Duncan GJ, Simkins TJ, Emery B. Neuron-Oligodendrocyte interactions in the structure and integrity of axons. Front Cell Dev Biology. 2021;9:653101.
44. Lei C, Chen H, Chen K. Effects of bone marrow mesenchymal stem cells on Myelin repair and emotional changes of a cuprizone-induced demyelination model. JIN. 2023;22(2):40.
45. Ngo V, Duennwald ML. Nrf2 and oxidative stress: a general overview of mechanisms and implications in human disease. Antioxid (Basel). 2022;11(12):2345.
46. Loboda A, Damulewicz M, Pyza E, Jozkowicz A, Dulak J. Role of Nrf2/HO-1 system in development, oxidative stress response and diseases: an evolutionarily conserved mechanism. Cell Mol Life Sci. 2016;73(17):3221–47.
47. Jena AB, Samal RR, Bhol NK, Duttaroy AK. Cellular Red-Ox system in health and disease: the latest update. Biomed Pharmacother. 2023;162:114606.
48. Shiri E, Pasbakhsh P, Borhani-Haghighi M, Alizadeh Z, Nekoonam S, Mojaverrostami S, et al. Mesenchymal stem cells ameliorate Cuprizone-Induced

demyelination by targeting oxidative stress and mitochondrial dysfunction. Cell Mol Neurobiol. 2021;41(7):1467–81.
49. Fouzder C, Mukhuty A, Kundu R. Kaempferol inhibits Nrf2 signalling pathway via downregulation of Nrf2 mRNA and induces apoptosis in NSCLC cells. Arch Biochem Biophys. 2021;697:108700.
50. Bennett ML, Viaene AN. What are activated and reactive glia and what is their role in neurodegeneration? Neurobiol Dis. 2021;148:105172.
51. Bhol NK, Bhanjadeo MM, Singh AK, Dash UC, Ojha RR, Majhi S, et al. The interplay between cytokines, inflammation, and antioxidants: mechanistic insights and therapeutic potentials of various antioxidants and anti-cytokine compounds. Biomed Pharmacother. 2024;178:117177.
52. Madadi S, Shiri E, Pasbakhsh P, Tahmasebi F, Kazemzadeh S, Zibara K, et al. Combination therapy of mesenchymal stem cell transplantation and astrocyte ablation improve remyelination in a Cuprizone-Induced demyelination mouse model. Mol Neurobiol. 2022;59(12):7278–92.
53. Li W-H, Cheng X, Yang Y-L, Liu M, Zhang S-S, Wang Y-H, et al. Kaempferol attenuates neuroinflammation and blood brain barrier dysfunction to improve neurological deficits in cerebral ischemia/reperfusion rats. Brain Res. 2019;1722:146361.
54. Pusic AD, Kraig RP. Youth and environmental enrichment generate serum exosomes containing miR-219 that promote CNS myelination. Glia. 2014;62(2):284–99.
55. Su H, Wang Z, Zhou L, Liu D, Zhang N. Regulation of the Nrf2/HO-1 axis by mesenchymal stem cells-derived extracellular vesicles: implications for disease treatment. Front Cell Dev Biol. 2024;12:1397954.
56. Xiao H, Yu X, Liu Y, Jiang W, Meng X, Dong Z, et al. Mesenchymal stem cell-derived exosomes–a promising therapeutic approach to improve neurocognitive disorders in chronic obstructive pulmonary disease. Stem Cell Res Ther. 2025;16:314.
57. Chen X-Q, Fawcett JR, Rahman Y-E, Ala TA, Frey WH. Delivery of nerve growth factor to the brain via the olfactory pathway. J Alzheimer's Disease. 1998;1(1):35–44.
58. Dhuria SV, Hanson LR, Frey IIWH. Intranasal delivery to the central nervous system: mechanisms and experimental considerations. J Pharm Sci. 2010;99(4):1654–73.
59. Zarei M, Mohammadi S, Jabbari S, Shahidi S. Intracerebroventricular microinjection of Kaempferol on memory retention of passive avoidance learning in rats: involvement of cholinergic mechanism (s). Int J Neurosci. 2019;129(12):1203–12.
60. Kouhestani S, Jafari A, Babaei P. Kaempferol attenuates cognitive deficit via regulating oxidative stress and neuroinflammation in an ovariectomized rat model of sporadic dementia. Neural Regeneration Res. 2018;13(10):1827–32.

Publisher's note